# Genetic Modifiers of Neurodegeneration in a *Drosophila* Model of Parkinson's Disease

**Sierra Lavoy,[*,†,‡] Vinita G. Chittoor-Vinod,[*,†,‡] Clement Y. Chow,[§] and Ian Martin[*,†,‡,1]**
[*]Jungers Center for Neurosciences, [†]Department of Neurology, and [‡]Parkinson Center of Oregon, Oregon Health and Science University, Portland, Oregon 97239, and [§]Department of Human Genetics, University of Utah School of Medicine, Salt Lake City, Utah

**ABSTRACT** Disease phenotypes can be highly variable among individuals with the same pathogenic mutation. There is increasing evidence that background genetic variation is a strong driver of disease variability in addition to the influence of environment. To understand the genotype–phenotype relationship that determines the expressivity of a pathogenic mutation, a large number of backgrounds must be studied. This can be efficiently achieved using model organism collections such as the *Drosophila* Genetic Reference Panel (DGRP). Here, we used the DGRP to assess the variability of locomotor dysfunction in a LRRK2 G2019S *Drosophila melanogaster* model of Parkinson's disease (PD). We find substantial variability in the LRRK2 G2019S locomotor phenotype in different DGRP backgrounds. A genome-wide association study for candidate genetic modifiers reveals 177 genes that drive wide phenotypic variation, including 19 top association genes. Genes involved in the outgrowth and regulation of neuronal projections are enriched in these candidate modifiers. RNAi functional testing of the top association and neuronal projection-related genes reveals that *pros*, *pbl*, *ct*, and *CG33506* significantly modify age-related dopamine neuron loss and associated locomotor dysfunction in the *Drosophila* LRRK2 G2019S model. These results demonstrate how natural genetic variation can be used as a powerful tool to identify genes that modify disease-related phenotypes. We report novel candidate modifier genes for LRRK2 G2019S that may be used to interrogate the link between LRRK2, neurite regulation and neuronal degeneration in PD.

**KEYWORDS** Parkinson's disease; LRRK2; dopamine neurons; *D. melanogaster*

PARKINSON'S disease (PD) is an age-associated neurodegenerative disease of unknown cause. Established therapeutic approaches provide symptomatic relief, but do not modify the underlying disease (Hardy *et al.* 2006). Recently, the contribution of genetic and epigenetic factors to PD development has been increasingly recognized (Trinh and Farrer 2013). This follows the identification of pathogenic mutations in genes including *SNCA* (*Synuclein alpha*), *LRRK2 (leucine-rich repeat kinase 2)*, *PINK1 (PTEN-induced putative kinase 1)*, *parkin*, and *DJ-1*, along with numerous risk susceptibility loci found in idiopathic PD via genome-wide association studies (Hardy *et al.* 2006; Trinh and Farrer 2013). LRRK2, which is linked to autosomal-dominant familial PD, has received much attention because (i) LRRK2-linked familial PD clinically and pathologically recapitulates late-onset idiopathic disease, (ii) the disease-causing G2019S mutation and multiple risk variants at the LRRK2 locus are prevalent in idiopathic PD, and (iii) targeting the functional kinase activity of LRRK2 is a promising therapeutic approach (West 2015). At least some pathogenic mutations, including the common G2019S mutation, enhance LRRK2 kinase activity and blocking kinase activity pharmacologically or genetically prevents LRRK2 neurotoxicity *in vitro* and in animal models (West *et al.* 2005, 2007; Greggio *et al.* 2006; Smith *et al.* 2006; Jaleel *et al.* 2007; Luzon-Toro *et al.* 2007; Imai *et al.* 2008; Anand *et al.* 2009; Covy and Giasson 2009; Kumar *et al.* 2010; Lee *et al.* 2010; Angeles *et al.* 2011; Webber *et al.* 2011; Matta *et al.* 2012; Biosa *et al.* 2013; Martin *et al.* 2014; Reynolds *et al.* 2014; Silva *et al.* 2014). While aberrant LRRK2 kinase activity has been shown to affect a number of processes including cytoskeletal regulation (Parisiadou *et al.* 2009; Lin *et al.* 2010; Chan *et al.* 2011; Kawakami *et al.* 2012; Sepulveda *et al.* 2013; Civiero *et al.* 2015), vesicular trafficking (Matta *et al.* 2012; MacLeod *et al.* 2013; Steger *et al.* 2016),


doi: https://doi.org/10.1534/genetics.118.301119
Manuscript received May 7, 2018; accepted for publication June 3, 2018; published Early Online June 15, 2018.
Supplemental material available at Figshare: https://doi.org/10.25386/genetics.6229304.
[1]Corresponding author: Jungers Center for Neurosciences Research, Parkinson Center of Oregon, Department of Neurology, Mail Code L623, Oregon Health and Science University, 3181 SW Sam Jackson Park Rd., Portland, OR 97239. E-mail: martiia@ohsu.edu

autophagy (Plowey *et al.* 2008; Alegre-Abarrategui *et al.* 2009; Tong *et al.* 2010, 2012; Xiong *et al.* 2010; Herzig *et al.* 2011; Korolchuk and Rubinsztein 2011; Korolchuk *et al.* 2011; Ahmed *et al.* 2012; Friedman *et al.* 2012; Orenstein *et al.* 2013; Su and Qi 2013; Schapansky *et al.* 2014), mitochondrial function (Saha *et al.* 2009; Niu *et al.* 2012; Wang *et al.* 2012; Su and Qi 2013), and protein synthesis (Imai *et al.* 2008; Gehrke *et al.* 2010; Martin *et al.* 2014), precisely how LRRK2 mutations cause neuronal death remains unclear. Ultimately, prevention of LRRK2 pathogenesis will likely require a detailed understanding of the key mechanisms driving neurodegeneration. The clinical and pathological overlap between LRRK2-linked PD and idiopathic PD supports the notion that this understanding will have broad impact on our insight into PD even beyond cases where LRRK2 mutations are involved.

Penetrance of the LRRK2 G2019S mutation is incomplete even at advanced age, with estimates ranging from 25 to 80% and possibly varying among different ethnic populations (Healy *et al.* 2008; Hulihan *et al.* 2008; Sierra *et al.* 2011; Marder *et al.* 2015; Trinh *et al.* 2016; Lee *et al.* 2017). While some of this incomplete penetrance may be due to environmental factors, it is likely that background genetic variation impacts the probability of a LRRK2 G2019S carrier developing disease. Genetic variation can be harnessed as a powerful tool to identify which genes modify disease outcomes (Satake *et al.* 2009; Simón-Sánchez *et al.* 2009; Gandhi and Wood 2010; Nalls *et al.* 2014; Pickrell *et al.* 2016). This can be achieved effectively and efficiently using animal disease models when appropriate genetic tools and disease-relevant traits are available for study (Threadgill *et al.* 2011; Churchill *et al.* 2012; Mackay *et al.* 2012; Grenier *et al.* 2015). In *Drosophila*, for example, flies expressing human LRRK2 G2019S exhibit an age-dependent loss of dopamine neurons leading to pronounced locomotor deficits (Liu *et al.* 2008; Martin *et al.* 2014). Importantly, flies expressing human wild-type LRRK2 do not exhibit similar PD-related phenotypes, supporting the existence of mutation-specific effects (Liu *et al.* 2008; Martin *et al.* 2014). To determine the effects of genetic variation on LRRK2 G2019S-associated locomotor deficits, we used the *Drosophila* Genetic Reference Panel (DGRP), a large set of genetically-diverse background strains with fully sequenced genomes (Mackay *et al.* 2012). This panel has successfully been used to identify genetic modifiers in a number of diseases, infection, and cell stress models (Carbone *et al.* 2009; Jordan *et al.* 2012; Chow *et al.* 2013, 2016; He *et al.* 2014). We hypothesized that by assessing the effect of natural genetic variation on the LRRK2 G2019S locomotor phenotype that correlates with neurodegeneration in *Drosophila*, we could identify new candidate modifier genes that would provide important insights into the principle mechanisms underlying neuronal death.

## Materials and Methods

### *Drosophila stocks and culture*

The 148 DGRP lines used in the study (Supplemental Material, Table S3) were obtained from the Bloomington *Drosophila* Stock Center. The *UAS-LRRK2-G2019S* and *UAS-LRRK2* lines have been characterized elsewhere (Liu *et al.* 2008; Martin *et al.* 2014) and were a gift from W. Smith. The double transgenic *Ddc-GAL4*; *UAS-LRRK2-G2019S* and *Ddc-GAL4*; *UAS-LRRK2* lines were created using *Ddc-GAL4* from the Bloomington *Drosophila* Stock Center (line 7010). Lines carrying RNAi constructs under UAS enhancer control were from the Bloomington *Drosophila* stock center (line numbers in parenthesis): *mAChR-C* (61306), *CG6420* (36088), *CG9003* (31362), *Eip63E* (34075), *IP3K2* (55240), *Khc-73* (38191), *nonC* (31094), *zfh1* (43195), *chi* (31049), *ct* (29625), *kon* (31584), *kay* (31322), *kn* (31916), *pbl* (28343), *pros* (26745) *smal* (55907) and control (36303) or Vienna *Drosophila* RNAi Center (line number in parenthesis): *CG12224* (31700), *CG14355* (109776), *CG14881* (110294), *CG17565* (110646), *CG33506* (107235), *Tie* (26879), *wry* (8021), *cv-c* (100247), *tup* (45859) and control (60100). All flies were reared and aged at 25°/60% relative humidity under a 12-hr light-dark cycle on standard cornmeal medium.

### *Negative geotaxis*

***DGRP screening:*** Cohorts of 75–100 female flies (0–3 days old, selecting against flies with visible signs of recent eclosion) collected from crosses between *Ddc-GAL4*; *UAS-LRRK2-G2019S* or *Ddc-GAL4*; *UAS-LRRK2*, and each of 148 DGRP genetic backgrounds or $w^{1118}$ were collected under brief anesthesia and transferred to fresh food vials to recover (25 flies/vial). Female *Ddc-GAL4*; *UAS-LRRK2-G2019S* expressing flies were used as they exhibit more pronounced locomotor deficits than males. We reasoned that, for candidate suppressors, this would allow for a finer assessment of degree of suppression. Flies were aged for 6 weeks with transfer to fresh food twice per week. After 2 weeks, flies were transferred to empty vials, allowed 1 min to rest and then tapped to the bottom of the vial three times within a 1 sec interval to initiate climbing. The position of each fly was captured in a digital image 4 sec after climbing initiation using a fixed camera. Flies were then returned to their original food vial. Flies were subsequently tested again with the same protocol after a total of 6 weeks of aging. Automated image analysis was performed on digital images using the particle analysis tool on Scion Image to derive *x*–*y* coordinates for each fly thus providing the height climbed, as previously described (Gargano *et al.* 2005). The performance of flies in a single vial was calculated from the average height climbed by all flies in that vial to generate a single datum ($N = 1$). Performance of each line was then derived from the average scores of 3–4 vials tested for the line ($N = 3–4$).

***RNAi screening:*** For testing effects of candidate modifiers on LRRK2 G2019S phenotypes, *Ddc-GAL4*; *UAS-LRRK2-G2019S* flies were crossed to each RNAi line. Additionally, *Ddc-GAL4*; *UAS-LRRK2-G2019S* or *UAS-LRRK2-G2019S* flies were crossed to an RNAi background line. For testing the effects of RNAi in the absence of LRRK2 G2019S, *Ddc-GAL4* flies were crossed to each RNAi line or to an RNAi background line. Cohorts of 75–100 female flies (0–3 days old selecting against flies with visible signs of recent eclosion) were collected under brief anesthesia and transferred to fresh food vials to recover (25 flies/vial). Flies were aged for 2 and 6 weeks and negative geotaxis performance was measured as described above. Performance of TRiP and VDRC controls crossed to *Ddc-GAL4*; *UAS-LRRK2-G2019S* were almost identical and, as the majority of RNAi stocks are from the TRiP collection, that RNAi control is shown.

### *Dopamine neuron viability*

*Ddc-GAL4*; *UAS-LRRK2-G2019S* flies were crossed to each RNAi line. *Ddc-GAL4*; *UAS-LRRK2-G2019S* or *UAS-LRRK2-G2019S* flies were crossed to an RNAi background line. Cohorts of 50 male and female flies (0–3 days old) were collected under brief anesthesia and transferred to fresh food vials to recover (25 flies/vial). Flies were aged for 6 weeks then brains were harvested, fixed, and permeabilized. Immunohistochemistry for tyrosine hydroxylase (TH)-expressing neurons was performed using methods described elsewhere (Wu and Luo 2006). Briefly, after blocking the brains in 5% normal goat serum/0.3% PBS-T, brains were incubated in anti-TH antibody (Immunostar) for two nights at 4° on a nutator. Brains were washed extensively, then incubated in alexa-fluor 488 anti-mouse secondary antibody for two nights at 4° on a nutator. Brains were washed extensively, mounted, and imaged on a Zeiss LSM710 confocal microscope. Confocal z-stacks were acquired at 1 μm slice intervals. In order to quantify dopamine neurons, projection images through the brain to capture PAL (protocerebral anterior lateral), PPM1/2 (protocerebral posterior medial 1/2), PPM3, PPL1 (protocerebral posterior lateral 1) and PPL2 clusters were generated.

### *Cytoscape functional network analysis of candidate modifier genes*

Gene enrichment was assessed using the Cytoscape plug-in ClueGO, searching for GO molecular function and biological process terms. *P* values for group and term enrichment are calculated by Fisher Exact Test and corrected by Bonferroni step-down.

### *Genome-wide association*

Association analysis was performed as previously described (Chow *et al.* 2016). DGRP genotypes were downloaded from the website, http://dgrp.gnets.ncsu.edu/. Variants were filtered for minor allele frequency (≥0.05), and nonbiallelic sites were removed. A total of 1,866,414 SNPs were included in the analysis. Negative geotaxis score for 148 DGRP/LRRK2 G2019S or 142 DGRP/LRRK2 (wildtype) F1 progeny were regressed on each SNP. To account for cryptic relatedness (He *et al.* 2014), GEMMA (v. 0.94) (Zhou and Stephens 2012) was used to both estimate a centered genetic relatedness matrix and perform association tests using the following linear mixed model (LMM):

$$\boldsymbol{y} = \alpha + \boldsymbol{x}\beta + \boldsymbol{u} + \epsilon$$

$$\boldsymbol{u} \sim MVN_n\left(0, \lambda\tau^{-1}\mathbf{K}\right)$$

$$\epsilon \sim MVN_n\left(0, \tau^{-1}\mathbf{I}_n\right)$$

where, as described and adapted from Zhou and Stephens (2012), $y$ is the $n$-vector of negative geotaxis scores for the $n$ lines, $\alpha$ is the intercept, $x$ is the $n$-vector of marker genotypes, and $\beta$ is the effect size of the marker. $u$ is a $n \times n$ matrix of random effects with a multivariate normal distribution ($MVN_n$) that depends on $\lambda$, the ratio between the two variance components, $\tau^{-1}$, the variance of residuals errors, and, where the covariance matrix is informed by K, the calculated $n \times n$ marker-based relatedness matrix. K accounts for all pairwise nonrandom sharing of genetic material among lines, $\epsilon$ is a $n$-vector of residual errors, with a multivariate normal distribution that depends on $\tau^{-1}$, and $I_n$, the identity matrix. Quantile-quantile (Q-Q) plot analysis indicated an appropriate fit to the LMM (Figure S3). Genes were identified from SNP coordinates using the BDGP R54/dm3 genome build. A SNP was assigned to a gene if it was within the gene's transcription boundaries or no more than 1000 bp upstream/downstream of those boundaries.

### *Statistical analysis*

Unless otherwise described in the methods, data were analyzed by ANOVA with Bonferroni correction for multiple comparisons.

### *Data availability*

SNP location data in the DGRP collection (Freeze 2.0 calls) are archived on the GSA Figshare portal and can additionally be downloaded from the DGRP data portal (http://dgrp2.gnets.ncsu.edu/data/website/dgrp2.tgeno). Supplemental material available at Figshare: https://doi.org/10.25386/genetics.6229304.

## Results

### *Locomotor dysfunction in LRRK2 G2019S flies is affected by genetic background*

Flies expressing pathogenic LRRK2 G2019S via the dopaminergic *Ddc-GAL4* driver exhibit an age-dependent loss of dopamine neurons, with accompanying deficits in locomotor function (Liu *et al.* 2008; Martin *et al.* 2014). We crossed the LRRK2 G2019S mutation into the suite of DGRP fly lines in order to examine the effect of natural genetic background variation on age-related locomotor dysfunction induced by mutant LRRK2. Double transgenic flies (*Ddc-GAL4*; *UAS-LRRK2-G2019S*) were crossed to 148 DGRP lines to produce F1 progeny deriving half of their genetic background from the parental DGRP line, permitting the assessment of dominant background effects on the LRRK2 G2019S locomotor phenotype.

In a $w^{1118}$ background, LRRK2 G2019S locomotor deficits are absent in young flies and manifest at ~6 weeks of age (Martin *et al.* 2014). We aged F1 progeny for 6 weeks and measured performance in negative geotaxis longitudinally at 2- and 6-weeks of age (Figure 1). DGRP background has a strong effect on locomotor performance at both ages, (2 weeks, $P < 1.08 \times 10^{-66}$; 6 weeks, $P < 4.04 \times 10^{-44}$) and there is a significant interaction between age and DGRP background effects on geotaxis performance ($P < 0.0001$), suggesting that the DGRP genetic backgrounds result in a distinct effect on locomotor performance in aged animals where G2019S locomotor deficits have previously been observed (Liu *et al.* 2008; Martin *et al.* 2014). As, to our knowledge, the DGRP genetic backgrounds have not previously been tested for age-related locomotor function, we considered the possibility that variability in DGRP line locomotor performance could be due to the effects of aging on the different DGRP backgrounds, and, thus, could occur independently of the LRRK2 G2019S mutation. To directly assess this, we carried out a control experiment in which the DGRP genetic background lines were crossed to a wildtype LRRK2-expressing line (*Ddc-GAL4*; *UAS-LRRK2*). F1 progeny from these crosses were aged for 6 weeks and tested for locomotor performance as the DGRP/LRRK2 G2019S lines were. The results reveal poor correlation between DGRP line means from the wildtype LRRK2 F1 progeny and the LRRK2 G2019S F1 progeny (Figure S1). Hence, the effect of genetic background on locomotor performance does not occur independently of LRRK2 G2019S.

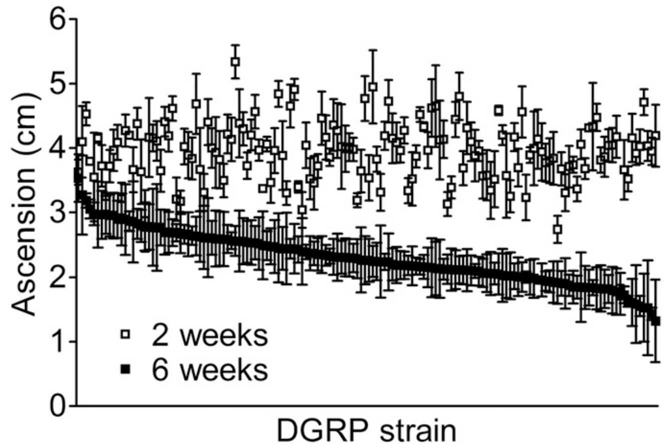


**Figure 1** Locomotor function of LRRK2 G2019S flies depends on genetic background. Negative geotaxis of *Ddc-GAL4*; *UAS-LRRK2-G2019S* flies in 148 DGRP backgrounds at 2 and 6 weeks of age. DGRP background has a strong effect on locomotor performance at both ages (2 weeks, $P < 1.08 \times 10^{-66}$; 6 weeks, $P < 4.04 \times 10^{-44}$).

### *Genome-wide association reveals candidate modifiers of LRRK2 G2019S locomotor dysfunction*

The large range of geotaxis scores seen in LRRK2 G2019S flies with different DGRP backgrounds suggests that genetic variation influences mutant LRRK2-mediated locomotor dysfunction. Quantitative geotaxis scores of aged flies (6 weeks old) were used to test for association with genome-wide single nucleotide polymorphisms (SNPs) in an unbiased manner. We tested whether a given SNP was associated with the LRRK2 G2019S locomotor phenotype using a genome-wide association approach. With a large number of SNPs (1,866,414) tested over just 148 lines, the study was not sufficiently powered for SNP associations to survive multiple testing correction. However, our goal was not to treat these associations as being definitive, but to use these SNPs to nominate candidate modifier genes for subsequent functional validation. This approach yields a number of genes that potentially underlie the variable expressivity of LRRK2 G2019S phenotypes for further testing.

In total, 177 candidate genes collectively harboring 280 SNPs are associated with variability in the LRRK2 G2019S locomotor phenotype at a *P*-value threshold of $P < 10^{-5}$ (Table S1). A subset of 19 genes (with 31 associated SNPs) meet the more restrictive nominal *P*-value threshold of $P < 10^{-6}$, and can therefore be considered top candidates by statistical association (Table 1). These genes are hereafter referred to as top association candidates. There were no common GWAS candidate genes nominated by the wildtype LRRK2 and LRRK2 G2019S data sets when considering SNPs associated at a P # 1026 threshold (Table 2). Within this group, for LRRK2 G2019S 15 genes have human orthologs (Table 1), and several genes harbor multiple associated SNPs (four in *wry* and two each in *CG43277* and *tie*). These genes cover a broad range of annotated functions, including microtubule binding and motor activity for *Khc*-73 (Huckaba *et al.* 2011), motor neuron axon guidance for *zfh1* (Layden *et al.* 2006; Zarin *et al.* 2014), notch signaling for *wry* (Kim *et al.* 2010), and calcium signaling for *IP3K2* (Lloyd-Burton *et al.* 2007). *KIF13A*, one of the putative human orthologs of *Khc-73*, is reported to play a role in the trafficking of mannose-6-phosphate-containing vesicles from the *trans*-Golgi to the plasma membrane (Nakagawa *et al.* 2000). This is notable given the proposed role for LRRK2 in regulating vesicular trafficking through its interaction with Rabs (MacLeod *et al.* 2013; Steger *et al.* 2016). A gene ontology enrichment analysis on all 177 candidates revealed an enrichment of genes within a number of functional groups, the most significant being dendrite guidance ($P = 2.9 \times 10^{-6}$) and regulation of cell projection organization ($P = 3.0 \times 10^{-5}$) (Table S2). These findings are striking considering the recognized role of LRRK2 in regulating neurite outgrowth as well as the loss of neurite complexity consistently reported in cultured neurons or animals expressing LRRK2 G2019S (MacLeod *et al.* 2006; Rajput *et al.* 2006; Parisiadou *et al.* 2009; Lin *et al.* 2010; Chan *et al.* 2011; Dusonchet *et al.* 2011; Kawakami *et al.* 2012, 2014; Sepulveda *et al.* 2013; Civiero *et al.* 2015; Schwab and Ebert 2015; Tsika *et al.* 2015). Collectively, we termed genes from the dendrite guidance and regulation of cell projection GO categories as neuron projection candidates (Table 3). None of these candidates fall within the top association genes. Performing gene enrichment analysis exclusively on the list of top

**Table 1 Top association candidate genes**

| Rank | SNP[a] | Candidate gene(s) | *P*-value | FDR | Human ortholog | OMIM |
|---|---|---|---|---|---|---|
| 1 | 3R:9973680 | *CG14355* | $2.65E^{-07}$ | 0.37 | – | – |
| 2 | 2R:10746081 | *CG33506* | $3.99E^{-07}$ | 0.37 | *TMEM177* | – |
| 3 | 2R:15525692 | *CG43277*[b] | $2.46E^{-06}$ | 0.47 | – | – |
| 4 | 2R:11417294 | *Khc-73* | $2.87E^{-06}$ | 0.47 | *KIF13A/KIF13B* | 605433/607350 |
| 5 | X:14035579 | *CR44658*[b] | $3.17E^{-06}$ | 0.47 | – | – |
| 6 | 3R:26611553 | *zfh1* | $3.69E^{-06}$ | 0.47 | *ZEB2* | 605802 |
| 7 | 2L:1844384 | *wry* | $4.10E^{-06}$ | 0.47 | *DNER* | 607299 |
| 8 | 3L:4510450 | *Tie* | $4.12E^{-06}$ | 0.47 | *TEK/Tie1* | 600221/600222 |
| 9 | X:13199667 | *IP3K2* | $4.41E^{-06}$ | 0.47 | *ITPKA/ITPKB* | 147521 |
| 10 | 3R:22549408 | *CG6420* | $5.15E^{-06}$ | 0.47 | *WDR20* | – |
| 11 | 3R:7806766 | *CG12224* | $5.38E^{-06}$ | 0.47 | *KCNAB2* | 601142 |
| 12 | 3R:12260571 | *CG17565/CG14881* | $6.16E^{-06}$ | 0.47 | *FNTB/ARMC7* | 134636 |
| 13 | 3R:13196662 | *CR44256*[b] | $6.31E^{-06}$ | 0.47 | – | – |
| 14 | 3L:3521221 | *Eip63E* | $7.42E^{-06}$ | 0.47 | *CDK14* | 610679 |
| 15 | X:6727165 | *nonC/mAChR-C* | $7.58E^{-06}$ | 0.47 | *SMG1/GPR119* | 607032/300513 |
| 16 | 2R:7528497 | *CG9003* | $7.61E^{-06}$ | 0.47 | *FBXL20* | 609086 |
| 17 | 3R:18824405 | *Nha2*[b] | $8.20E^{-06}$ | 0.49 | *SLC9B1/SLC9B2* | 611527 |

[a] SNP with most statistically significant association for the candidate gene.
[b] No RNAi line available for testing candidate gene.

association genes does not give any functional enrichment, which is not surprising given that there are only 19 genes.

### *Targeted knock-down of candidate genes impacts LRRK2 G2019S neurodegeneration*

In order to test the candidate modifier genes nominated by our initial screen, we pursued the top association candidates and neuron projection candidates (25 genes total) to test their ability to influence the LRRK2 G2019S locomotor phenotype. Inclusion of the neuron projection candidates was on the basis of compelling functional evidence linking LRRK2 G2019S to altered neurite morphology (MacLeod *et al.* 2006; Rajput *et al.* 2006; Parisiadou *et al.* 2009; Lin *et al.* 2010; Chan *et al.* 2011; Dusonchet *et al.* 2011; Kawakami *et al.* 2012, 2014; Sepulveda *et al.* 2013; Civiero *et al.* 2015; Schwab and Ebert 2015; Tsika *et al.* 2015) as well as our hypothesis that we may identify novel modifiers of LRRK2 G2019S-mediated neurodegeneration that could provide insight into pathogenesis. We used RNAi to probe whether lowering candidate gene expression influenced the LRRK2 G2019S locomotor phenotype. RNAi lines for each candidate were mated to *Ddc-GAL4*; *UAS-LRRK2-G2019S* flies to generate progeny with concomitant LRRK2 G2019S expression and candidate modifier knock-down (KD) in dopamine neurons. RNAi lines were available for all candidates except two nonprotein-coding genes (*CR44658* and *CR44256*), *CG43277* and *nha-2*. Although this simple loss-of-function approach does not fully assess the contribution of each gene to the phenotype, it allows us to directly probe for a phenotype modifying effect of candidate gene KD specifically within dopamine neurons while using readily available genetic tools.

As with the initial genetic screen, we assessed the LRRK2 G2019S locomotor phenotype by measuring negative geotaxis in 2- and 6-week-old flies. RNAi for *CG9003*, *cv-c* and *kn* each result in reduced geotaxis performance in 2-week-old flies, raising the possibility that they may impact locomotor function independently of LRRK2 G2019S (Figure 2). Indeed, *Ddc-GAL4* driven KD of these three candidate genes without LRRK2 G2019S expression induce locomotor dysfunction in aged flies (Figure S2). Knocking down 7 of the 15 top association candidates tested (47%) significantly enhances LRRK2 G2019S locomotor deficits at 6 weeks of age (*mAChR-C*, *CG14355*, *CG14881*, *CG17565*, *CG33506*, *CG9003*, and *tie*). None of the 15 top association candidates tested suppressed the LRRK2 G2019S locomotor phenotype when knocked down. RNAi for 6 of the 10 neuron projection candidates (60%) significantly affects the LRRK2 G2019S phenotype at 6 weeks of age (Figure 2). Of these six, five candidates (*cv-c*, *kn*, *pbl*, *pros* and *tup*) enhance and one candidate (*ct*) suppresses the phenotype when knocked-down.

To test whether a significant candidate modifier KD effect on the LRRK2 G2019S locomotor phenotype correlates with a change in neuronal degeneration, we next examined dopamine neuron viability in aged flies for the RNAi lines which modified locomotor performance in aged LRRK2 G2019S flies, but which had no effect in the absence of LRRK2 G2019S. Hence, *CG9003*, *cv-c*, and *kn* were not advanced to this stage of testing. We assessed five dopamine neuron clusters (PAL, PPM1/2, PPM3, PPL1, and PPL2) in the fly brain that are readily quantifiable. Most of the top association candidates have a modest effect on dopamine neuron viability; the only candidate reaching statistical significance is *CG33506*, which is the second highest ranked candidate based on SNP association. While LRRK2 G2019S expression alone causes a 20% loss of dopamine neurons for the five clusters counted, additional *CG33506* KD leads to a 43% decrease. This correlates well with locomotor effects, where geotaxis scores decrease by 25% with LRRK2 G2019S expression alone and 54% with additional *CG33506* KD. *CG33506* is uncharacterized, although reported to be expressed in fly heads (Aradska *et al.*

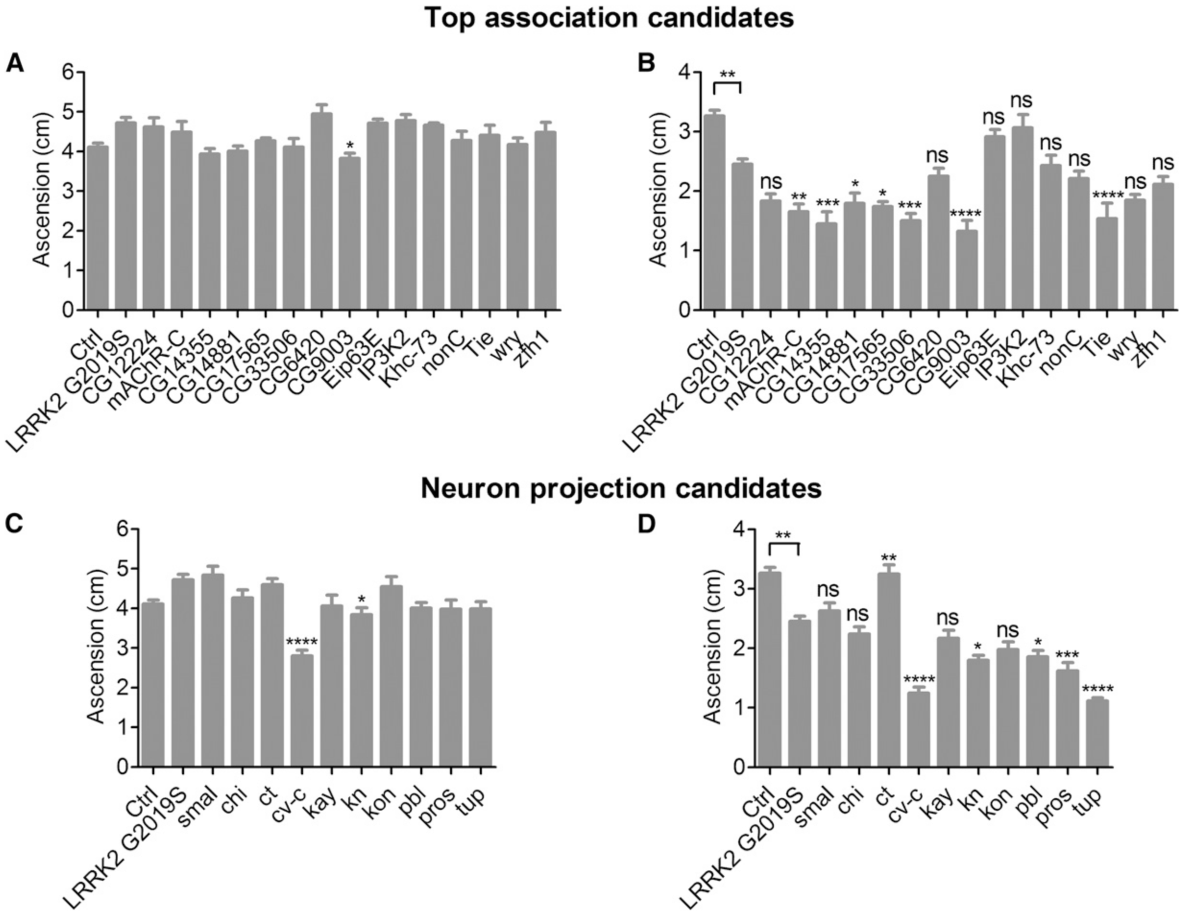


**Figure 2** Effect of candidate modifier gene KD on LRRK2 G2019S locomotor dysfunction. Top association candidates were tested at 2 weeks (A) and 6 weeks (B) of age. Neuron projection candidates were tested at 2 weeks (C) and 6 weeks (D) of age. In each case, there was a significant effect of genotype on geotaxis (individual ANOVAs, $P < 0.0006$). In 6-week-old flies, Bonferroni post-tests revealed a significant effect of G2019S LRRK2 expression and an enhancement or suppression effect of RNAi for some candidate genes on the performance of G2019S LRRK2-expressing flies (ns not significant, * $P < 0.05$, ** $P < 0.01$, *** $P < 0.001$, **** $P < 0.0001$). Ctrl is +/+; *UAS-LRRK2-G2019S*/+ and LRRK2 G2019S is *Ddc-GAL4*/+; *UAS-LRRK2-G2019S*/+.

2015). The human ortholog of *CG33506* is *TMEM177*, which has 42.1% identity at the nucleotide level and 25.3% identity at the protein level. TMEM177 is a multi-pass transmembrane protein, largely uncharacterized but expressed throughout the body, including in brain, and thought to localize to mitochondria (Calvo *et al.* 2016). From our neuron projection candidates subject to dopamine neuron assessment, three out of four of the RNAi lines exhibit a significant modifier effect on neuronal viability (Figure 3). In accordance with their effects on the LRRK2 G2019S locomotor phenotype, both *pros* and *pbl* enhance loss of dopamine neurons upon KD, while *ct* suppresses it. KD of *tup* also enhances LRRK2 G2019S-mediated dopamine neuron death consistent with its effects on geotaxis performance, although the difference did not reach statistical significance. All three neuron projection candidates that significantly modify both locomotor and dopamine neuron phenotypes when knocked-down have human homologs and established roles in neurite morphogenesis. While RNAi effects on locomotor function and dopamine neuron viability in LRRK2 G2019S flies generally correlate, it should be noted that KD of three genes (*mAChR-C*, *tie* and *CG14355*; 30% of candidates tested) produce non-significant effects on dopamine neuron viability that do not correspond directionally with their effects on geotaxis (Figure 3).

## Discussion

Genetic background can be an important factor in determining whether disease manifests in an individual harboring a given pathogenic mutation. LRRK2 G2019S penetrance is age-related but incomplete even by the eighth decade (Healy *et al.* 2008; Hulihan *et al.* 2008; Latourelle *et al.* 2008; Sierra *et al.* 2011; Trinh and Farrer 2013; Marder *et al.* 2015; Lee *et al.* 2017). Environmental and genetic factors are both likely to play a role in determining whether a LRRK2 G2019S carrier develops PD. In *Drosophila*, the impact of natural genetic variation on a given trait can be assessed in an unbiased manner using established genetic tools such as the DGRP suite of flies. The DGRP facilitates assessment of quantifiable

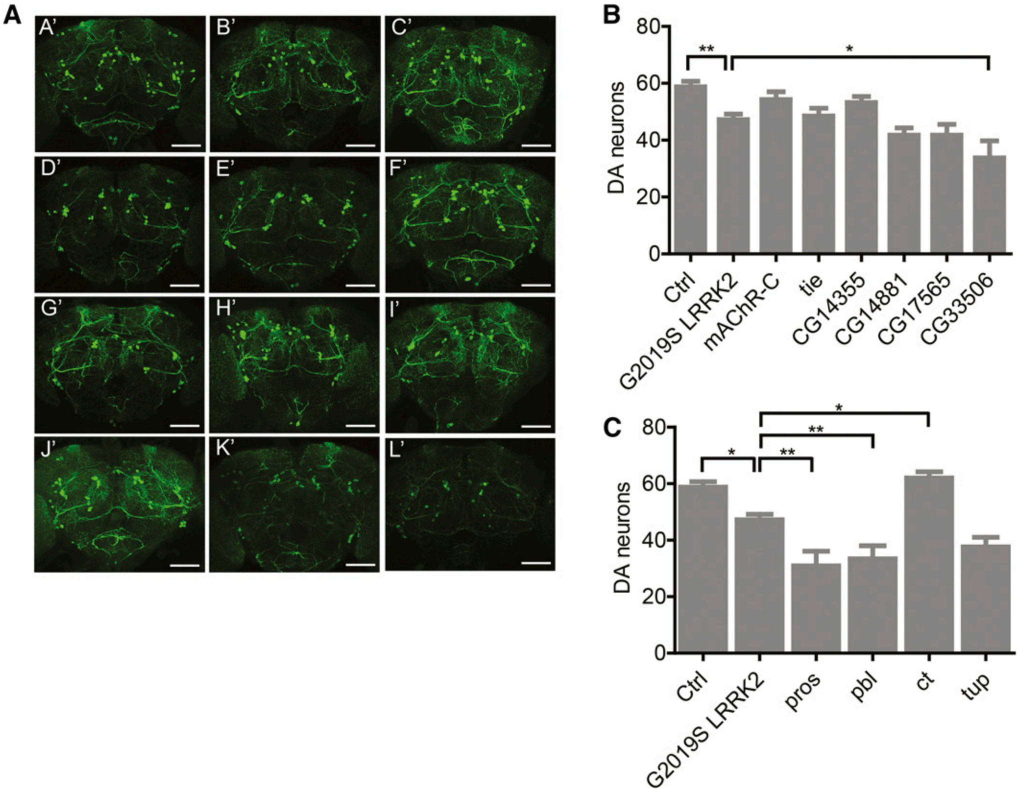


**Figure 3** Effect of candidate modifier gene KD on LRRK2 G2019S dopamine neuron loss. (A) Confocal projection images through the brain of control +/+; UAS-LRRK2-G2019S/+ (A′), and *Ddc-GAL4*/+; *UAS-LRRK2-G2019S*/+ (B′) flies and G2019S LRRK2 expressing flies with RNAi-mediated knockdown of mAChR-C (C′), tie (D′), CG14355 (E′), CG14881 (F′), CG17565 (G′), CG33506 (H′), pros (I′), pbl (J′), ct (K′) and tup (L′). Bar, 60 μM. Quantitation of total dopamine neurons in five clusters (PPM1/2, PPM3, PPL1, PPL2, and PAL) for top association (B) and neuron projection (C) candidate genes. There was a significant effect of genotype for both (individual ANOVAs, $P < 0.0001$) and Bonferroni post-tests revealed a significant effect of G2019S LRRK2 expression and KD of *CG33506*, *pros*, *pbl* and *ct* candidate modifiers (* $P < 0.05$, ** $P < 0.01$).

phenotypes in a large number of fully-sequenced backgrounds, and has been used on numerous occasions to demonstrate variation in disease-relevant traits (Jordan *et al.* 2012; Mackay *et al.* 2012; Weber *et al.* 2012; Chow *et al.* 2013, 2016; He *et al.* 2014; Park *et al.* 2014; Wang *et al.* 2017). We used the DGRP to show that genetic background strongly influences the age-related locomotor phenotype seen in LRRK2 G2019S expressing flies, and identified candidate modifier genes of mutant LRRK2. Our unbiased genome-wide association study identified numerous SNPs associated with the LRRK2 G2019S locomotor phenotype. Importantly, the genes nominated may affect the LRRK2 G2019S locomotor phenotype not just as downstream mediators of LRRK2 neurotoxicity, but also as upstream regulators of LRRK2 expression/function or by acting in parallel pathways that functionally converge with LRRK2 to influence dopamine neuron integrity. As anticipated, there was no strong correlation between the DGRP line effects at 2 weeks and at 6 weeks of age in our study (Figure 1). Genetic background can have distinct influences on locomotor performance in young and aged flies, manifest as a relatively high-performing background at 2 weeks that becomes a relatively low-performing background at 6 weeks, or vice versa (Martin and Grotewiel 2006). This is likely due to distinct, and in some cases even opposing effects of genetic background on performance vigor in young flies and on age-related changes that occur over this large portion of the fly life span.

Our GWAS relies on the association of many SNPs over just 148 lines, which for the locomotor phenotype analysis performed did not enable sufficient power to identify definitive SNPs with very high association that survive multiple testing correction. Since this increases the possibility of identifying false-positives, we used the SNPs simply to nominate candidate modifier genes for subsequent detailed validation. Based on this simple goal, we did not examine the molecular nature of the associated SNPs in terms of how they might impact expression or function of candidate genes. The vast majority of SNPs in these candidate genes were noncoding and therefore it is difficult to predict how they may impact expression levels. Further, obtaining definitive evidence to address this question would require experimental testing of the SNPs and gene function, which was beyond the goals of the study.

Considering the possibility that phenotypic variability in the DGRP backgrounds could occur independently of LRRK2 G2019S, and alternatively be related to effects of the different backgrounds or LRRK2 overexpression on age-related negative geotaxis behavior, we tested a separate cohort of F1 progeny using the same genetic backgrounds but this time expressing wild type LRRK2. This revealed poor correlation between the DGRP backgrounds expressing LRRK2 with those expressing LRRK2 G2019S (Figure S1). We further performed a GWAS on the wild-type LRRK2 cohort, deriving a total of 12 top association candidates (at $P \leq 10^{-6}$), none of which overlapped with the top association candidates obtained via a LRRK2 G2019S GWAS (Table 1 and Table 2). These lines of evidence argue that the phenotypic variability observed via LRRK2 G2019S is not simply due to effects of the DGRP

**Table 2 Wild type LRRK2 top association candidate genes**

| Rank | SNP[a] | Candidate gene | *P*-value | Human ortholog | OMIM |
|---|---|---|---|---|---|
| 1 | 3L:10050040 | *dpr6* | $3.88E^{-07}$ | — | — |
| 2 | 3L:21397373 | *rgn* | $1.49E^{-06}$ | REG1A | 167770 |
| 3 | 3R:27842339 | *CR45557* | $1.58E^{-06}$ | — | — |
| 4 | 3R:27651356 | *RhoGAP100F* | $1.90E^{-06}$ | SYDE1 | 617377 |
| 5 | X:18889282 | *CG43759* | $2.37E^{-06}$ | — | — |
| 6 | X:19061795 | *Inx5* | $3.91E^{-06}$ | — | — |
| 7 | 2R:8429948 | *fra* | $4.70E^{-06}$ | NEO1 | 601907 |
| 8 | 2R:13961559 | *CG34386* | $7.87E^{-06}$ | — | — |
| 9 | X:9100745 | *SmydA-9* | $7.97E^{-06}$ | SMYD2 | 610663 |
| 10 | 2R:15036909 | *ena* | $8.37E^{-06}$ | ENAH | 609061 |
| 11 | 3R:27805736 | *heph* | $9.65E^{-06}$ | PTBP1 | 600693 |
| 12 | X:5248137 | *sk* | $9.86E^{-06}$ | — | — |

[a] SNP with most statistically significant association for the candidate gene.

backgrounds or LRRK2 expression on age-related locomotor performance and is dependent on mutant LRRK2 G2019S expression. Attempting to undertake a joint analysis in which the deviation in performance between LRRK2 and LRRK2 G2019S for each genetic background forms a basis for GWAS analysis was precluded by the testing of each F1 progeny cohort separately. A complex behavioral phenotype such as negative geotaxis is prone to cohort effects caused by environmental variables that occur over the course of aging. These additional variables confound the ability to meaningfully isolate "mutation-specific" effects by subtracting performance scores between two cohorts that are reared, aged and tested separately. These possible cohort effects could in theory also impact the correlation analysis of DGRP backgrounds expressing LRRK2 *vs.* LRRK2 G2019S, yet likely not in a manner that would prevent our ability to observe a strong correlation between the two sets. Additionally, while we were not able to incorporate an integrated analysis of this nature, the approach we took by performing a GWAS directly on the LRRK2 G2019S cohort is supported by the subsequent testing and observation that 13 out of 25 top association and neuron projection candidates nominated by this GWAS were validated as modifiers of locomotor function in aged LRRK2 G2019S flies (Table 3). Hence, we are confident that our approach has led to the identification of authentic LRRK2 G2019S phenotype modifiers that warrant further investigation.

Among the list of genes nominated by genome-wide association, we prioritized for further testing a subset of candidates with the strongest statistical association, and those in two enriched GO categories (dendrite guidance and regulation of cell projection organization) where direct relevance to LRRK2 function is supported by prior studies. By considering not only our top association hits but also gene ontology-enriched candidates associated at $P < 10^{-5}$, we hoped to partially overcome the lack of statistical power for identifying definitive candidates based on SNP associations. This approach led to a pool of potential targets for which subsequent validation permitted identification of LRRK2 G2019S genetic modifiers of high confidence. Knocking down 13 out of these 25 candidates significantly modifies the LRRK2 G2019S locomotor phenotype in aged flies, and, after subsequent testing of dopamine neuron viability, we derived a final set of candidate genes: *CG33506*, *pros*, *pbl*, and *ct* that significantly modify both locomotor dysfunction and dopamine neuron loss phenotypes of LRRK2 G2019S in *Drosophila*. That we were ultimately able to identify a set of candidate modifier genes for both locomotor and dopamine neuron viability phenotypes supports the GWAS study in terms of the targets nominated by this approach. *pros* is a transcriptional regulator involved in neuronal differentiation and is required for axon and dendrite development. *pbl* is a Rho guanine nucleotide exchange factor (GEF) involved in a number of processes including axonogenesis. *ct* is a homeoprotein transcription factor known to influence dendritic morphology in fly dendritic arborization neurons. A role for LRRK2 in regulating neurite outgrowth has been documented through the interaction with proteins important in cytoskeletal dynamics such as Rac1, PAK6, ERM proteins, MARK1 and Tau as well as the cytoskeletal proteins Actin and Tubulin themselves (Parisiadou *et al.* 2009; Lin *et al.* 2010; Chan *et al.* 2011; Dusonchet *et al.* 2011; Kawakami *et al.* 2012, 2014; Sepulveda *et al.* 2013; Civiero *et al.* 2015; Schwab and Ebert 2015; Tsika *et al.* 2015). These studies show that cytoskeletal protein interactions may be perturbed by the G2019S mutation leading to neuronal injury *in vitro*. Our study reinforces this relationship, and crucially goes further by demonstrating a direct link between genes important for neurite development/maintenance and DA neurodegenerative phenotypes *in vivo*. Further, we have identified novel candidate interactors for LRRK2 that, through further characterization, may help delineate the precise mechanism by which LRRK2 regulates neurite morphogenesis.

It is currently hard to hypothesize how *CG33506* (human ortholog *TMEM177*) may be involved in LRRK2 biology or neurodegeneration. TMEM177 is thought to localize to mitochondrial membranes where protein interaction mapping suggests an interaction with numerous mitochondrial ribosomal proteins (Calvo *et al.* 2016). Our previous work shows that LRRK2 impacts bulk protein synthesis which contributes to LRRK2 G2019S neurodegeneration through unclear mechanisms (Martin *et al.* 2014), but whether it affects mitochondrial protein synthesis is unknown. Mutations in another multi-pass transmembrane protein TMEM230 were recently associated with familial PD (Deng *et al.* 2016). TMEM230 did not colocalize with a mitochondria marker but is thought to localize to vesicles and impact synaptic vesicle trafficking (Deng *et al.* 2016). Considering this and the broad range of functions encompassed by transmembrane proteins, it is unclear whether TMEM177 and TMEM230 have any connection relevant to LRRK2.

Marcogliese *et al.* (2017) recently conducted a genetic screen to identify modifiers of LRRK2 I2020T eye degeneration in *Drosophila*. They initially screened through deficiency lines (containing deletions that cover almost the entire genome) at 25 and 29° in flies expressing I2020T LRRK2 via the eye-specific *GMR-GAL4* driver, followed by functional testing

**Table 3 Neuron projection candidate genes**

| Candidate gene | SNP[a] | *P*-value | Human ortholog | OMIM |
|---|---|---|---|---|
| *chi* | 2R:19919006 | $1.67E^{-05}$ | – | – |
| *ct* | X:7535575 | $6.06E^{-05}$ | *CUX1/CUX2* | 116896/610648 |
| *cv-c* | 3R:10260649 | $7.42E^{-05}$ | *DLC1* | 604258 |
| *kay* | 3R:25611636 | $7.16E^{-05}$ | *FOS/FOSL1/FOSL2* | 164810/136515/601575 |
| *kn* | 2R:10671765 | $9.12E^{-05}$ | *EBF3* | 607407 |
| *kon* | 2L:18491720 | $6.20E^{-05}$ | *CSPG4* | 601172 |
| *pbl* | 3L:7905741 | $1.48E^{-05}$ | *ECT2* | 600586 |
| *pros* | 3R:7155471 | $6.68E^{-05}$ | *PROX1* | 601546 |
| *smal* | 2L:6187849 | $4.05E^{-05}$ | *DDR1/DDR2* | 600408/191311 |
| *tup* | 2L:18863703 | $1.83E^{-05}$ | *ISL1* | 600366 |

[a] SNP with most statistically significant association for the candidate gene.

of candidate modifiers. Their set of final candidate modifiers validated to impact dopamine neuron viability in addition to eye degeneration does not overlap with our candidates that modify both age-related locomotor dysfunction and dopamine neuron loss. One simple explanation for this is that modifiers for different pathogenic variants of LRRK2 may be distinct, although both G2019S and I2020T mutations are thought to be neurotoxic at least in part through an elevation of LRRK2 kinase activity (West *et al.* 2005). One possible explanation for this is that as a starting point, they expressed LRRK2 I2020T in the eye and used an eye degeneration phenotype for their screen while we expressed in LRRK2 G2019S in dopamine neurons and used an age-related locomotor phenotype that is directly related to dopamine neuron loss. We believe our approach has the advantage that age-related locomotor dysfunction due to dopamine neuron loss is potentially more directly related to PD than eye degeneration phenotypes. The higher consistency of effects on locomotor and dopamine neuron phenotypes in our study would also suggest this. Of the 10 candidates selected for dopamine neuron viability assessment in our study, six candidates (60%) affected both phenotypes in the same direction, whereas 6 out of 16 candidates (38%) showed consistent effects in their I2020T LRRK2 study. As noted by the authors, the dichotomy in directional effects between eye degeneration and dopamine neuron loss encountered may have been caused by false positive results in their initial screen.

Our findings highlight the influence of natural genetic variation in the expressivity of disease-related phenotypes. The DGRP has been successfully utilized to uncover the impact of genetic background variation on traits linked to retinitis pigmentosa and resistance to infection (Wang *et al.* 2017), along with cellular responses to ER stress (Chow *et al.* 2013) and oxidative stress (Weber *et al.* 2012). We have now extended this to locomotor deficits in a model of PD and additionally identified novel candidate modifier genes for a disease pathway relevant to LRRK2. Effective prevention of neuronal death resulting from LRRK2 mutations will require a detailed understanding of the key mechanisms driving neurodegeneration. This study generates new targets to investigate and may direct future studies on LRRK2 pathobiology and therapeutic intervention in PD.

## Acknowledgments

We thank the Advanced Light Microscopy Core for subsidized confocal microscope use. This work was supported by National Institutes of Health (NIH) (P30NS061800) to the Oregon Health and Science University (OHSU) Advanced Light Microscopy Core, support to I.M. from the Parkinson Center of Oregon and OHSU Neurology Foundation Funds. C.Y.C. was supported by an NIH/ National Institute of General Medical Sciences (NIGMS) Maximizing Investigators' Research Award (1R35GM124780), a University of Utah Seed Grant, and a Glenn Foundation Award for Research in Biological Mechanisms of Aging. C.Y.C. is the Mario R. Capecchi Endowed Chair in Genetics.

## Literature Cited

Ahmed, I., Y. Liang, S. Schools, V. L. Dawson, T. M. Dawson *et al.*, 2012 Development and characterization of a new Parkinson's disease model resulting from impaired autophagy. J. Neurosci. 32: 16503–16509. https://doi.org/10.1523/JNEUROSCI.0209-12.2012

Alegre-Abarrategui, J., H. Christian, M. M. Lufino, R. Mutihac, L. L. Venda *et al.*, 2009 LRRK2 regulates autophagic activity and localizes to specific membrane microdomains in a novel human genomic reporter cellular model. Hum. Mol. Genet. 18: 4022–4034. https://doi.org/10.1093/hmg/ddp346

Anand, V. S., L. J. Reichling, K. Lipinski, W. Stochaj, W. Duan *et al.*, 2009 Investigation of leucine-rich repeat kinase 2: enzymological properties and novel assays. FEBS J. 276: 466–478. https://doi.org/10.1111/j.1742-4658.2008.06789.x

Angeles, D. C., B. H. Gan, L. Onstead, Y. Zhao, K. L. Lim *et al.*, 2011 Mutations in LRRK2 increase phosphorylation of peroxiredoxin 3 exacerbating oxidative stress-induced neuronal death. Hum. Mutat. 32: 1390–1397. https://doi.org/10.1002/humu.21582

Aradska, J., T. Bulat, F. J. Sialana, R. Birner-Gruenberger, B. Erich *et al.*, 2015 Gel-free mass spectrometry analysis of *Drosophila melanogaster* heads. Proteomics 15: 3356–3360. https://doi.org/10.1002/pmic.201500092

Biosa, A., A. Trancikova, L. Civiero, L. Glauser, L. Bubacco *et al.*, 2013 GTPase activity regulates kinase activity and cellular

phenotypes of Parkinson's disease-associated LRRK2. Hum. Mol. Genet. 22: 1140–1156. https://doi.org/10.1093/hmg/dds522
Calvo, S. E., K. R. Clauser, and V. K. Mootha, 2016 MitoCarta2.0: an updated inventory of mammalian mitochondrial proteins. Nucleic Acids Res. 44: D1251–D1257. https://doi.org/10.1093/nar/gkv1003
Carbone, M. A., J. F. Ayroles, A. Yamamoto, T. V. Morozova, S. A. West *et al.*, 2009 Overexpression of myocilin in the *Drosophila* eye activates the unfolded protein response: implications for glaucoma. PLoS One 4: e4216. https://doi.org/10.1371/journal.pone.0004216
Chan, D., A. Citro, J. M. Cordy, G. C. Shen, and B. Wolozin, 2011 Rac1 protein rescues neurite retraction caused by G2019S leucine-rich repeat kinase 2 (LRRK2). J. Biol. Chem. 286: 16140–16149. https://doi.org/10.1074/jbc.M111.234005
Chow, C. Y., M. F. Wolfner, and A. G. Clark, 2013 Using natural variation in *Drosophila* to discover previously unknown endoplasmic reticulum stress genes. Proc. Natl. Acad. Sci. USA 110: 9013–9018. https://doi.org/10.1073/pnas.1307125110
Chow, C. Y., K. J. Kelsey, M. F. Wolfner, and A. G. Clark, 2016 Candidate genetic modifiers of retinitis pigmentosa identified by exploiting natural variation in *Drosophila*. Hum. Mol. Genet. 25: 651–659. https://doi.org/10.1093/hmg/ddv502
Churchill, G. A., D. M. Gatti, S. C. Munger, and K. L. Svenson, 2012 The diversity outbred mouse population. Mamm. Genome 23: 713–718. https://doi.org/10.1007/s00335-012-9414-2
Civiero, L., M. D. Cirnaru, A. Beilina, U. Rodella, I. Russo *et al.*, 2015 Leucine-rich repeat kinase 2 interacts with p21-activated kinase 6 to control neurite complexity in mammalian brain. J. Neurochem. 135: 1242–1256. https://doi.org/10.1111/jnc.13369
Covy, J. P., and B. I. Giasson, 2009 Identification of compounds that inhibit the kinase activity of leucine-rich repeat kinase 2. Biochem. Biophys. Res. Commun. 378: 473–477. https://doi.org/10.1016/j.bbrc.2008.11.048
Deng, H. X., Y. Shi, Y. Yang, K. B. Ahmeti, N. Miller *et al.*, 2016 Identification of TMEM230 mutations in familial Parkinson's disease. Nat. Genet. 48: 733–739. https://doi.org/10.1038/ng.3589
Dusonchet, J., O. Kochubey, K. Stafa, S. M. Young, Jr., R. Zufferey *et al.*, 2011 A rat model of progressive nigral neurodegeneration induced by the Parkinson's disease-associated G2019S mutation in LRRK2. J. Neurosci. 31: 907–912. https://doi.org/10.1523/JNEUROSCI.5092-10.2011
Friedman, L. G., M. L. Lachenmayer, J. Wang, L. He, S. M. Poulose *et al.*, 2012 Disrupted autophagy leads to dopaminergic axon and dendrite degeneration and promotes presynaptic accumulation of alpha-synuclein and LRRK2 in the brain. J. Neurosci. 32: 7585–7593. https://doi.org/10.1523/JNEUROSCI.5809-11.2012
Gandhi, S., and N. W. Wood, 2010 Genome-wide association studies: the key to unlocking neurodegeneration? Nat. Neurosci. 13: 789–794. https://doi.org/10.1038/nn.2584
Gargano, J. W., I. Martin, P. Bhandari, and M. S. Grotewiel, 2005 Rapid iterative negative geotaxis (RING): a new method for assessing age-related locomotor decline in *Drosophila*. Exp. Gerontol. 40: 386–395. https://doi.org/10.1016/j.exger.2005.02.005
Gehrke, S., Y. Imai, N. Sokol, and B. Lu, 2010 Pathogenic LRRK2 negatively regulates microRNA-mediated translational repression. Nature 466: 637–641. https://doi.org/10.1038/nature09191
Greggio, E., S. Jain, A. Kingsbury, R. Bandopadhyay, P. Lewis *et al.*, 2006 Kinase activity is required for the toxic effects of mutant LRRK2/dardarin. Neurobiol. Dis. 23: 329–341. https://doi.org/10.1016/j.nbd.2006.04.001
Grenier, J. K., J. R. Arguello, M. C. Moreira, S. Gottipati, J. Mohammed *et al.*, 2015 Global diversity lines - a five-continent reference panel of sequenced *Drosophila melanogaster* strains. G3 (Bethesda) 5: 593–603. https://doi.org/10.1534/g3.114.015883
Hardy, J., H. Cai, M. R. Cookson, K. Gwinn-Hardy, and A. Singleton, 2006 Genetics of Parkinson's disease and parkinsonism. Ann. Neurol. 60: 389–398. https://doi.org/10.1002/ana.21022
He, B. Z., M. Z. Ludwig, D. A. Dickerson, L. Barse, B. Arun *et al.*, 2014 Effect of genetic variation in a *Drosophila* model of diabetes-associated misfolded human proinsulin. Genetics 196: 557–567. https://doi.org/10.1534/genetics.113.157800
Healy, D. G., M. Falchi, S. S. O'Sullivan, V. Bonifati, A. Durr *et al.*, 2008 Phenotype, genotype, and worldwide genetic penetrance of LRRK2-associated Parkinson's disease: a case-control study. Lancet Neurol. 7: 583–590. https://doi.org/10.1016/S1474-4422(08)70117-0
Herzig, M. C., C. Kolly, E. Persohn, D. Theil, T. Schweizer *et al.*, 2011 LRRK2 protein levels are determined by kinase function and are crucial for kidney and lung homeostasis in mice. Hum. Mol. Genet. 20: 4209–4223. https://doi.org/10.1093/hmg/ddr348
Huckaba, T. M., A. Gennerich, J. E. Wilhelm, A. H. Chishti, and R. D. Vale, 2011 Kinesin-73 is a processive motor that localizes to Rab5-containing organelles. J. Biol. Chem. 286: 7457–7467. https://doi.org/10.1074/jbc.M110.167023
Hulihan, M. M., L. Ishihara-Paul, J. Kachergus, L. Warren, R. Amouri *et al.*, 2008 LRRK2 Gly2019Ser penetrance in Arab-Berber patients from Tunisia: a case-control genetic study. Lancet Neurol. 7: 591–594. https://doi.org/10.1016/S1474-4422(08)70116-9
Imai, Y., S. Gehrke, H. Q. Wang, R. Takahashi, K. Hasegawa *et al.*, 2008 Phosphorylation of 4E-BP by LRRK2 affects the maintenance of dopaminergic neurons in *Drosophila*. EMBO J. 27: 2432–2443. https://doi.org/10.1038/emboj.2008.163
Jaleel, M., R. J. Nichols, M. Deak, D. G. Campbell, F. Gillardon *et al.*, 2007 LRRK2 phosphorylates moesin at threonine-558: characterization of how Parkinson's disease mutants affect kinase activity. Biochem. J. 405: 307–317. https://doi.org/10.1042/BJ20070209
Jordan, K. W., K. L. Craver, M. M. Magwire, C. E. Cubilla, T. F. Mackay *et al.*, 2012 Genome-wide association for sensitivity to chronic oxidative stress in *Drosophila melanogaster*. PLoS One 7: e38722. https://doi.org/10.1371/journal.pone.0038722
Kawakami, F., T. Yabata, E. Ohta, T. Maekawa, N. Shimada *et al.*, 2012 LRRK2 phosphorylates tubulin-associated tau but not the free molecule: LRRK2-mediated regulation of the tau-tubulin association and neurite outgrowth. PLoS One 7: e30834. https://doi.org/10.1371/journal.pone.0030834
Kawakami, F., N. Shimada, E. Ohta, G. Kagiya, R. Kawashima *et al.*, 2014 Leucine-rich repeat kinase 2 regulates tau phosphorylation through direct activation of glycogen synthase kinase-3beta. FEBS J. 281: 3–13. https://doi.org/10.1111/febs.12579
Kim, I. M., M. J. Wolf, and H. A. Rockman, 2010 Gene deletion screen for cardiomyopathy in adult *Drosophila* identifies a new notch ligand. Circ. Res. 106: 1233–1243. https://doi.org/10.1161/CIRCRESAHA.109.213785
Korolchuk, V. I., and D. C. Rubinsztein, 2011 Regulation of autophagy by lysosomal positioning. Autophagy 7: 927–928. https://doi.org/10.4161/auto.7.8.15862
Korolchuk, V. I., S. Saiki, M. Lichtenberg, F. H. Siddiqi, E. A. Roberts *et al.*, 2011 Lysosomal positioning coordinates cellular nutrient responses. Nat. Cell Biol. 13: 453–460. https://doi.org/10.1038/ncb2204
Kumar, A., E. Greggio, A. Beilina, A. Kaganovich, D. Chan *et al.*, 2010 The Parkinson's disease associated LRRK2 exhibits weaker in vitro phosphorylation of 4E-BP compared to autophosphorylation. PLoS One 5: e8730. https://doi.org/10.1371/journal.pone.0008730

Latourelle, J. C., M. Sun, M. F. Lew, O. Suchowersky, C. Klein *et al.*, 2008 The Gly2019Ser mutation in LRRK2 is not fully penetrant in familial Parkinson's disease: the GenePD study. BMC Med. 6: 32. https://doi.org/10.1186/1741-7015-6-32

Layden, M. J., J. P. Odden, A. Schmid, A. Garces, S. Thor *et al.*, 2006 Zfh1, a somatic motor neuron transcription factor, regulates axon exit from the CNS. Dev. Biol. 291: 253–263. https://doi.org/10.1016/j.ydbio.2005.12.009

Lee, A. J., Y. Wang, R. N. Alcalay, H. Mejia-Santana, R. Saunders-Pullman *et al.*, 2017 Penetrance estimate of LRRK2 p.G2019S mutation in individuals of non-Ashkenazi Jewish ancestry. Mov. Disord. 32: 1432–1438. https://doi.org/10.1002/mds.27059

Lee, B. D., J. H. Shin, J. VanKampen, L. Petrucelli, A. B. West *et al.*, 2010 Inhibitors of leucine-rich repeat kinase-2 protect against models of Parkinson's disease. Nat. Med. 16: 998–1000. https://doi.org/10.1038/nm.2199

Lin, C. H., P. I. Tsai, R. M. Wu, and C. T. Chien, 2010 LRRK2 G2019S mutation induces dendrite degeneration through mislocalization and phosphorylation of tau by recruiting autoactivated GSK3β. J. Neurosci. 30: 13138–13149. https://doi.org/10.1523/JNEUROSCI.1737-10.2010

Liu, Z., X. Wang, Y. Yu, X. Li, T. Wang *et al.*, 2008 A *Drosophila* model for LRRK2-linked parkinsonism. Proc. Natl. Acad. Sci. USA 105: 2693–2698. https://doi.org/10.1073/pnas.0708452105

Lloyd-Burton, S. M., J. C. Yu, R. F. Irvine, and M. J. Schell, 2007 Regulation of inositol 1,4,5-trisphosphate 3-kinases by calcium and localization in cells. J. Biol. Chem. 282: 9526–9535. https://doi.org/10.1074/jbc.M610253200

Luzon-Toro, B., E. Rubio de la Torre, A. Delgado, J. Perez-Tur, and S. Hilfiker, 2007 Mechanistic insight into the dominant mode of the Parkinson's disease-associated G2019S LRRK2 mutation. Hum. Mol. Genet. 16: 2031–2039. https://doi.org/10.1093/hmg/ddm151

Mackay, T. F., S. Richards, E. A. Stone, A. Barbadilla, J. F. Ayroles *et al.*, 2012 The *Drosophila melanogaster* Genetic Reference Panel. Nature 482: 173–178. https://doi.org/10.1038/nature10811

MacLeod, D., J. Dowman, R. Hammond, T. Leete, K. Inoue *et al.*, 2006 The familial Parkinsonism gene LRRK2 regulates neurite process morphology. Neuron 52: 587–593. https://doi.org/10.1016/j.neuron.2006.10.008

MacLeod, D. A., H. Rhinn, T. Kuwahara, A. Zolin, G. Di Paolo *et al.*, 2013 RAB7L1 interacts with LRRK2 to modify intraneuronal protein sorting and Parkinson's disease risk. Neuron 77: 425–439 (erratum: Neuron 77: 994). https://doi.org/10.1016/j.neuron.2012.11.033

Marcogliese, P. C., S. Abuaish, G. Kabbach, E. Abdel-Messih, S. Seang *et al.*, 2017 *LRRK2(I2020T)* functional genetic interactors that modify eye degeneration and dopaminergic cell loss in *Drosophila*. Hum. Mol. Genet. 26: 1247–1257. https://doi.org/10.1093/hmg/ddx030

Marder, K., Y. Wang, R. N. Alcalay, H. Mejia-Santana, M. X. Tang *et al.*, 2015 Age-specific penetrance of LRRK2 G2019S in the Michael J. Fox Ashkenazi Jewish LRRK2 Consortium. Neurology 85: 89–95. https://doi.org/10.1212/WNL.0000000000001708

Martin, I., and M. S. Grotewiel, 2006 Distinct genetic influences on locomotor senescence in *Drosophila* revealed by a series of metrical analyses. Exp. Gerontol. 41: 877–881. https://doi.org/10.1016/j.exger.2006.06.052

Martin, I., J. W. Kim, B. D. Lee, H. C. Kang, J. C. Xu *et al.*, 2014 Ribosomal protein s15 phosphorylation mediates LRRK2 neurodegeneration in Parkinson's disease. Cell 157: 472–485. https://doi.org/10.1016/j.cell.2014.01.064

Matta, S., K. Van Kolen, R. da Cunha, G. van den Bogaart, W. Mandemakers *et al.*, 2012 LRRK2 controls an EndoA phosphorylation cycle in synaptic endocytosis. Neuron 75: 1008–1021. https://doi.org/10.1016/j.neuron.2012.08.022

Nakagawa, T., M. Setou, D. Seog, K. Ogasawara, N. Dohmae *et al.*, 2000 A novel motor, KIF13A, transports mannose-6-phosphate receptor to plasma membrane through direct interaction with AP-1 complex. Cell 103: 569–581. https://doi.org/10.1016/S0092-8674(00)00161-6

Nalls, M. A., N. Pankratz, C. M. Lill, C. B. Do, D. G. Hernandez *et al.*, 2014 Large-scale meta-analysis of genome-wide association data identifies six new risk loci for Parkinson's disease. Nat. Genet. 46: 989–993. https://doi.org/10.1038/ng.3043

Niu, J., M. Yu, C. Wang, and Z. Xu, 2012 Leucine-rich repeat kinase 2 disturbs mitochondrial dynamics via Dynamin-like protein. J. Neurochem. 122: 650–658. https://doi.org/10.1111/j.1471-4159.2012.07809.x

Orenstein, S. J., S. H. Kuo, I. Tasset, E. Arias, H. Koga *et al.*, 2013 Interplay of LRRK2 with chaperone-mediated autophagy. Nat. Neurosci. 16: 394–406. https://doi.org/10.1038/nn.3350

Parisiadou, L., C. Xie, H. J. Cho, X. Lin, X. L. Gu *et al.*, 2009 Phosphorylation of ezrin/radixin/moesin proteins by LRRK2 promotes the rearrangement of actin cytoskeleton in neuronal morphogenesis. J. Neurosci. 29: 13971–13980. https://doi.org/10.1523/JNEUROSCI.3799-09.2009

Park, S. Y., M. Z. Ludwig, N. A. Tamarina, B. Z. He, S. H. Carl *et al.*, 2014 Genetic complexity in a *Drosophila* model of diabetes-associated misfolded human proinsulin. Genetics 196: 539–555. https://doi.org/10.1534/genetics.113.157602

Pickrell, J. K., T. Berisa, J. Z. Liu, L. Segurel, J. Y. Tung *et al.*, 2016 Detection and interpretation of shared genetic influences on 42 human traits. Nat. Genet. 48: 709–717 (erratum: Nat. Genet. 48: 1296). https://doi.org/10.1038/ng.3570

Plowey, E. D., S. J. Cherra, III, Y. J. Liu, and C. T. Chu, 2008 Role of autophagy in G2019S-LRRK2-associated neurite shortening in differentiated SH-SY5Y cells. J. Neurochem. 105: 1048–1056. https://doi.org/10.1111/j.1471-4159.2008.05217.x

Rajput, A., D. W. Dickson, C. A. Robinson, O. A. Ross, J. C. Dachsel *et al.*, 2006 Parkinsonism, Lrrk2 G2019S, and tau neuropathology. Neurology 67: 1506–1508. https://doi.org/10.1212/01.wnl.0000240220.33950.0c

Reynolds, A., E. A. Doggett, S. M. Riddle, C. S. Lebakken, and R. J. Nichols, 2014 LRRK2 kinase activity and biology are not uniformly predicted by its autophosphorylation and cellular phosphorylation site status. Front. Mol. Neurosci. 7: 54. https://doi.org/10.3389/fnmol.2014.00054

Saha, S., M. D. Guillily, A. Ferree, J. Lanceta, D. Chan *et al.*, 2009 LRRK2 modulates vulnerability to mitochondrial dysfunction in Caenorhabditis elegans. J. Neurosci. 29: 9210–9218. https://doi.org/10.1523/JNEUROSCI.2281-09.2009

Satake, W., Y. Nakabayashi, I. Mizuta, Y. Hirota, C. Ito *et al.*, 2009 Genome-wide association study identifies common variants at four loci as genetic risk factors for Parkinson's disease. Nat. Genet. 41: 1303–1307. https://doi.org/10.1038/ng.485

Schapansky, J., J. D. Nardozzi, F. Felizia, and M. J. LaVoie, 2014 Membrane recruitment of endogenous LRRK2 precedes its potent regulation of autophagy. Hum. Mol. Genet. 23: 4201–4214. https://doi.org/10.1093/hmg/ddu138

Schwab, A. J., and A. D. Ebert, 2015 Neurite aggregation and calcium dysfunction in iPSC-derived sensory neurons with Parkinson's disease-related LRRK2 G2019S mutation. Stem Cell Reports 5: 1039–1052. https://doi.org/10.1016/j.stemcr.2015.11.004

Sepulveda, B., R. Mesias, X. Li, Z. Yue, and D. L. Benson, 2013 Short- and long-term effects of LRRK2 on axon and dendrite growth. PLoS One 8: e61986. https://doi.org/10.1371/journal.pone.0061986

Sierra, M., I. Gonzalez-Aramburu, P. Sanchez-Juan, C. Sanchez-Quintana, J. M. Polo *et al.*, 2011 High frequency and reduced penetrance of LRRK2 G2019S mutation among Parkinson's

disease patients in Cantabria (Spain). Mov. Disord. 26: 2343–2346. https://doi.org/10.1002/mds.23965
Silva, R. G., K. F. Geoghegan, X. Qiu, and A. Aulabaugh, 2014 A continuous and direct assay to monitor leucine-rich repeat kinase 2 activity. Anal. Biochem. 450: 63–69. https://doi.org/10.1016/j.ab.2014.01.007
Simón-Sánchez, J., C. Schulte, J. M. Bras, M. Sharma, J. R. Gibbs *et al.*, 2009 Genome-wide association study reveals genetic risk underlying Parkinson's disease. Nat. Genet. 41: 1308–1312. https://doi.org/10.1038/ng.487
Smith, W. W., Z. Pei, H. Jiang, V. L. Dawson, T. M. Dawson *et al.*, 2006 Kinase activity of mutant LRRK2 mediates neuronal toxicity. Nat. Neurosci. 9: 1231–1233. https://doi.org/10.1038/nn1776
Steger, M., F. Tonelli, G. Ito, P. Davies, M. Trost *et al.*, 2016 Phosphoproteomics reveals that Parkinson's disease kinase LRRK2 regulates a subset of Rab GTPases. eLife 5: e12813. https://doi.org/10.7554/eLife.12813
Su, Y. C., and X. Qi, 2013 Inhibition of excessive mitochondrial fission reduced aberrant autophagy and neuronal damage caused by LRRK2 G2019S mutation. Hum. Mol. Genet. 22: 4545–4561. https://doi.org/10.1093/hmg/ddt301
Threadgill, D. W., D. R. Miller, G. A. Churchill, and F. P. de Villena, 2011 The collaborative cross: a recombinant inbred mouse population for the systems genetic era. ILAR J. 52: 24–31. https://doi.org/10.1093/ilar.52.1.24
Tong, Y., H. Yamaguchi, E. Giaime, S. Boyle, R. Kopan *et al.*, 2010 Loss of leucine-rich repeat kinase 2 causes impairment of protein degradation pathways, accumulation of alpha-synuclein, and apoptotic cell death in aged mice. Proc. Natl. Acad. Sci. USA 107: 9879–9884. https://doi.org/10.1073/pnas.1004676107
Tong, Y., E. Giaime, H. Yamaguchi, T. Ichimura, Y. Liu *et al.*, 2012 Loss of leucine-rich repeat kinase 2 causes age-dependent bi-phasic alterations of the autophagy pathway. Mol. Neurodegener. 7: 2. https://doi.org/10.1186/1750-1326-7-2
Trinh, J., and M. Farrer, 2013 Advances in the genetics of Parkinson disease. Nat. Rev. Neurol. 9: 445–454. https://doi.org/10.1038/nrneurol.2013.132
Trinh, J., E. K. Gustavsson, C. Vilarino-Guell, S. Bortnick, J. Latourelle *et al.*, 2016 DNM3 and genetic modifiers of age of onset in LRRK2 Gly2019Ser parkinsonism: a genome-wide linkage and association study. Lancet Neurol. 15: 1248–1256. https://doi.org/10.1016/S1474-4422(16)30203-4
Tsika, E., A. P. Nguyen, J. Dusonchet, P. Colin, B. L. Schneider *et al.*, 2015 Adenoviral-mediated expression of G2019S LRRK2 induces striatal pathology in a kinase-dependent manner in a rat model of Parkinson's disease. Neurobiol. Dis. 77: 49–61. https://doi.org/10.1016/j.nbd.2015.02.019
Wang, J. B., H. L. Lu, and R. J. St Leger, 2017 The genetic basis for variation in resistance to infection in the *Drosophila melanogaster* genetic reference panel. PLoS Pathog. 13: e1006260. https://doi.org/10.1371/journal.ppat.1006260
Wang, X., M. H. Yan, H. Fujioka, J. Liu, A. Wilson-Delfosse *et al.*, 2012 LRRK2 regulates mitochondrial dynamics and function through direct interaction with DLP1. Hum. Mol. Genet. 21: 1931–1944. https://doi.org/10.1093/hmg/dds003
Webber, P. J., A. D. Smith, S. Sen, M. B. Renfrow, J. A. Mobley *et al.*, 2011 Autophosphorylation in the leucine-rich repeat kinase 2 (LRRK2) GTPase domain modifies kinase and GTP-binding activities. J. Mol. Biol. 412: 94–110. https://doi.org/10.1016/j.jmb.2011.07.033
Weber, A. L., G. F. Khan, M. M. Magwire, C. L. Tabor, T. F. Mackay *et al.*, 2012 Genome-wide association analysis of oxidative stress resistance in *Drosophila melanogaster*. PLoS One 7: e34745. https://doi.org/10.1371/journal.pone.0034745
West, A. B., 2015 Ten years and counting: moving leucine-rich repeat kinase 2 inhibitors to the clinic. Mov. Disord. 30: 180–189. https://doi.org/10.1002/mds.26075
West, A. B., D. J. Moore, S. Biskup, A. Bugayenko, W. W. Smith *et al.*, 2005 Parkinson's disease-associated mutations in leucine-rich repeat kinase 2 augment kinase activity. Proc. Natl. Acad. Sci. USA 102: 16842–16847. https://doi.org/10.1073/pnas.0507360102
West, A. B., D. J. Moore, C. Choi, S. A. Andrabi, X. Li *et al.*, 2007 Parkinson's disease-associated mutations in LRRK2 link enhanced GTP-binding and kinase activities to neuronal toxicity. Hum. Mol. Genet. 16: 223–232. https://doi.org/10.1093/hmg/ddl471
Wu, J. S., and L. Luo, 2006 A protocol for dissecting *Drosophila melanogaster* brains for live imaging or immunostaining. Nat. Protoc. 1: 2110–2115. https://doi.org/10.1038/nprot.2006.336
Xiong, Y., C. E. Coombes, A. Kilaru, X. Li, A. D. Gitler *et al.*, 2010 GTPase activity plays a key role in the pathobiology of LRRK2. PLoS Genet. 6: e1000902. https://doi.org/10.1371/journal.pgen.1000902
Zarin, A. A., J. Asadzadeh, K. Hokamp, D. McCartney, L. Yang *et al.*, 2014 A transcription factor network coordinates attraction, repulsion, and adhesion combinatorially to control motor axon pathway selection. Neuron 81: 1297–1311. https://doi.org/10.1016/j.neuron.2014.01.038
Zhou, X., and M. Stephens, 2012 Genome-wide efficient mixed-model analysis for association studies. Nat. Genet. 44: 821–824. https://doi.org/10.1038/ng.2310

*Communicating editor: S. Chenoweth*